

NJC

Accepted Manuscript



This is an *Accepted Manuscript*, which has been through the Royal Society of Chemistry peer review process and has been accepted for publication.

Accepted Manuscripts are published online shortly after acceptance, before technical editing, formatting and proof reading. Using this free service, authors can make their results available to the community, in citable form, before we publish the edited article. We will replace this *Accepted Manuscript* with the edited and formatted *Advance Article* as soon as it is available.

You can find more information about *Accepted Manuscripts* in the [Information for Authors](#).

Please note that technical editing may introduce minor changes to the text and/or graphics, which may alter content. The journal's standard [Terms & Conditions](#) and the [Ethical guidelines](#) still apply. In no event shall the Royal Society of Chemistry be held responsible for any errors or omissions in this *Accepted Manuscript* or any consequences arising from the use of any information it contains.

Niobate nanoscroll composite with Fe₂O₃ particles at moderate conditions: Assembly and application research

Dewei Li, Qingjie Li, Jie. He^{*}, Lifang Hu, Jinsong Hu

School of Chemical Engineering, Anhui University of Science and Technology, Huainan, 232001, P. R. China.

Abstract: Fe₂O₃/Nb₆O₁₇ nanoscroll composite was successfully assembled by exfoliation-restacking method at moderate conditions. The as-prepared samples were characterized by X-ray powder diffraction (XRD), Laser Raman spectroscopy (LRS), Field emission scanning electron microscopy (FESEM), High-resolution transmission electron microscopy (HRTEM), N₂ adsorption-desorption measurement, Thermo-gravimetric analysis, and UV-visible diffuse reflectance spectroscopy (UV-vis DRS). The results show that nanoscroll composite owns larger specific surface area (114 m²·g⁻¹), stronger spectral response and excellent photodegradation activities for MB under visible light irradiation. There is an obvious interaction between host niobate nanoscrolls and guest oxide Fe₂O₃ nanoparticles. Fe₂O₃ nanoparticles are crosslinked to the niobate nanoscroll surface as proved by a blue-shifted Raman vibration at 953 cm⁻¹ and 897 cm⁻¹ being associated with terminal Nb-OH groups.

Keywords: Niobate nanoscroll; Transition metal oxide; Assembly mechanism; Interaction; Photodegradation

1. Introduction

Layered compound, one of new photocatalytic materials, has immense application. Since the unique layered structure and the exfoliated nature, it has also been widely used in construction composites as a well support, especially layered niobate and titanoniobate^[1-6]. K₄Nb₆O₁₇ (structure as shown in Fig.1), one of the earliest researched layered photocatalysts, is mostly employed as a

* Corresponding author. Tel: +86-554-6668520; Fax: +86-554-6668520.

E-mail address: jhe@aust.edu.cn

well support to fabricate composite photocatalyst^[7-10] due to the wide band gap. Owing to the nature of nanosheets to form nanoscrolls^[11], namely the asymmetrical top and bottom faces in each layer, various nanoscroll composites were fabricated. These mesoporous nanoscroll composites possess obvious higher photocatalytic activities than guest oxide nanoparticles or host layered niobates alone. Therefore, they become excellent photocatalytic functional materials for photodegradation of organic pollutants. Now, some guest nanoparticles are used to fabricate mesoporous niobate nanoscroll composites, such as Co, Ag, Rh₂O₃, CdTe, Fe₃O₄, Au-Fe₃O₄, CuO, Pt, IrO_x, etc^[12-19]. Less attention has been paid to investigate the assembly mechanism between host niobate and guest nanoparticles. Exfoliation-restacking technology, usually utilized to prepare composite materials with a moderate prepared conditions, is an excellent approach to construct new photocatalytic materials and enhance their photocatalytic efficiency via broadening the photoabsorption region and effectively separating photo-generated electrons and holes. Fe₂O₃ is a narrow band gap semiconductor with a band-gap energy 2.2 eV and it can be used as a ideal guest material to prepared photocatalysts with visible light response^[20]. To the authors' knowledge, the performance of nanoscroll composites Fe₂O₃/Nb₆O₁₇ prepared by exfoliation- restacking method has been rarely explored. The assembly mechanism of niobate nanoscrolls with oxide nanoparticles has been rarely reported so far.

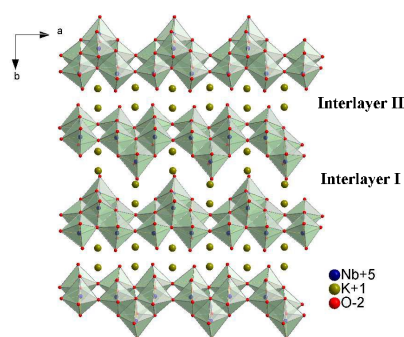


Fig.1 Structure diagram of K₄Nb₆O₁₇.

In the present study, the layered material K₄Nb₆O₁₇ was prepared by a solid state reaction method, and Nb₆O₁₇⁴⁻ nanosheet sols were obtained by ion exchange, exfoliation^[16]. Fe₂O₃ were employed as the guest oxide particles to fabricate niobate nanoscroll composites using exfoliation-restacking technology at moderate conditions, and their assembly mechanism was

proposed. The photocatalytic activities of the as-prepared composites $\text{Fe}_2\text{O}_3/\text{Nb}_6\text{O}_{17}$ were evaluated by the photodegradation of organic dye methylene blue in an aqueous solution.

2. Experimental

2.1 Preparation of Samples

The precursor $\text{K}_4\text{Nb}_6\text{O}_{17}$ was synthesized by heating the K_2CO_3 (AR, Sinopharm Chemical Reagent Co., Ltd) and Nb_2O_5 (2.5 N, Sinopharm Chemical Reagent Co., Ltd) mixture with the mole ratio of 2.3:3 in air at 1100 °C for 24 h. The as-obtained powder was washed by deionized water and then dried at 80 °C for 10 h. The $\text{H}_4\text{Nb}_6\text{O}_{17}$ was prepared by proton-exchanged process, which mixes 1 g $\text{K}_4\text{Nb}_6\text{O}_{17}$ with 30 mL 6 mol·L⁻³ HNO_3 (AR, Sinopharm Chemical Reagent Co., Ltd) aqueous solution at 333 K for a week and renew the acid solution every 24 h. Niobate nanosheet sols were obtained via following procedure: 1 g $\text{H}_4\text{Nb}_6\text{O}_{17}$ powder and 200 mL deionized water were added to beaker flask, the pH of suspension was adjusted to 9.5~10 with 25 % tetrabutylammonium hydroxide aqueous solution (N/A, Accela ChemBio Co., Ltd.). Then the mixture was oscillated at 45 °C for 3 days. Finally, the suspension was centrifugated at 8000 rpm to separate the nanosheets sols from the unexfoliated $\text{H}_4\text{Nb}_6\text{O}_{17}$ powders.

The $\text{Fe}(\text{OH})_3$ sols were obtained by hydrolyzing the FeCl_3 (AR, Sinopharm Chemical Reagent Co., Ltd) aqueous solution. The FeCl_3 solution was added dropwise to boiling water, boiled for 2-3 minutes after completion of the dropwise addition and then purified with semipermeable membrane (collodion membrane of artificial). Then the $\text{Fe}(\text{OH})_3$ sols were slowly dropped into the niobate nanosheet sols, with the Fe/Nb mole ratio of 1:1. After that, the suspension was oscillated continuously at room temperature for 12 h, 0.5 mol·L⁻¹ HNO_3 was slowly added until precipitation was completed. After aging for 48 h, the precipitate was separated by centrifugation and washed with ethanol and deionized water, dried in vacuum at 60 °C. The sample before calcination is assigned as B- $\text{Fe}_2\text{O}_3/\text{Nb}_6\text{O}_{17}$ and the sample after calcination in the resistance oven for 2 h at 400 °C is assigned as A- $\text{Fe}_2\text{O}_3/\text{Nb}_6\text{O}_{17}$. For comparison, pure Fe_2O_3 particles were prepared by drying and calcining the $\text{Fe}(\text{OH})_3$ sols at 400 °C for 2 h, respectively. The nanoscroll aggregates (assigned as NS- $\text{H}_4\text{Nb}_6\text{O}_{17}$) were obtained by dropwise adding 0.5 mol·L⁻¹ HNO_3 to the niobate nanosheet sols, then washed with deionized water and dried at 60 °C

for 48 h.

2.2 Characterization of Samples

The X-ray diffraction (XRD) patterns were recorded by using a XD-3 diffractometer (Beijing Purkinje General Instrument Co., Ltd.) with a curved graphite-monochromatied Cu-K α radiation ($\lambda= 1.5406\text{\AA}$) at 40 kV and 30 mA at room temperature. The Laser Raman spectra (LRS) were obtained on a Confocal Raman Microscope (InVia Reflex Spectrometer System, Renishaw) with a 785 nm wavelength of laser source. The UV-vis diffuse reflectance spectra (UV-vis DRS) were determined by TU-1901 UV-visible diffuse reflectance spectrometer (Beijing Purkinje General Instrument Co. Ltd.) equipped with an integrated sphere using BaSO₄ as the reference. The FESEM images were obtained by a Hitachi S-4800 field emission scanning electron microscope (Hitachi American Ltd.) with an acceleration voltage of 25 kV. HRTEM measurement was performed using JEOL JEM-2100 instrument that operated at an accelerating voltage of 200 KV with an EDAX Genesis energy-dispersive spectroscopy (EDS) system. The TG-DTA curves were measured by SDT2960 Simultaneous DSC-TGA (TA instrument, America) with a heating rate of 10 °C·min⁻¹ under nitrogen atmosphere. Nitrogen adsorption-desorption isotherms were obtained on a ASAP 2020 (Micromeritics instrument, America) at liquid-nitrogen temperature using nitrogen gas as the adsorbate, in which the samples were degassed at 100 °C for 24 h in flowing N₂ prior to the measurements.

2.3 Photocatalytic activity test

The photocatalytic activities of the as-prepared samples were evaluated by the photodegradation of organic dye methylene blue (MB, BS, Sinopharm Chemical Reagent Co., Ltd) aqueous solution under the visible light irradiation. A 300 W Xe lamp with a 400 nm cut-off filter was used as a light source. Methylene blue aqueous solutions (10 mg·L⁻¹) 200 mL and the as-prepared photocatalyst 20 mg were mixed in a quartz reactor. The mixtures were oscillated under dark conditions for 30 min to ensure adsorption equilibrium prior to light irradiation and kept under the same external conditions before and during the light irradiation. 3 mL mixtures were sampled at a given interval, and centrifugated to remove the photocatalyst at 9000 rpm. The supernatant was analyzed based on the absorption band maximum (664 nm) using a Shimadzu UV-2550 spectrometer.

3 Results and discussion

3.1 Thermal analysis of composites

Thermal analysis technology was used to investigate the thermal stability of the as-prepared materials. The TG-DTA curves of B-Fe₂O₃/Nb₆O₁₇ are showed in Fig.2. The total weight loss of B-Fe₂O₃/Nb₆O₁₇ nanocomposite is 12.5%. The weight loss below 200 °C is ca. 9% with a endothermic peak at 132 °C, which is attributed to the removal of the physically adsorbed water. The DTA curve exists a obvious endothermic peak at 316 °C which may be caused by the removal of bound water of interlayer. Taking into consideration that no obvious fluctuation was observed at 400-500 °C in the DTA-curve, dehydroxylation and dehydration of Fe(OH)₃ sols and the removal of crystal water or constitution water of the support nanoscrolls may be occurred meanwhile. Beyond 600 °C, it appears no distinct weight loss. An exothermic peak around 700 °C may have arisen from the structure collapse. So the calcination temperature for preparing the Fe₂O₃/Nb₆O₁₇ composite is determined at 400 °C for 2 h with a low heating rate of 2 °C · min⁻¹.

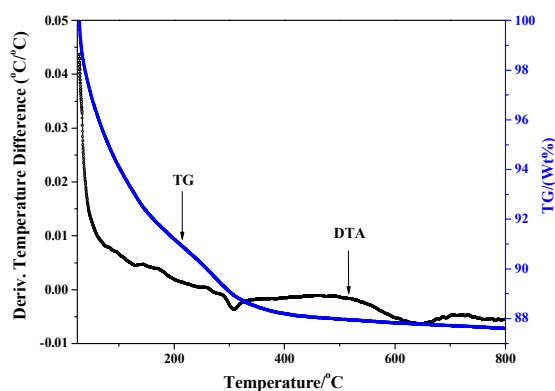
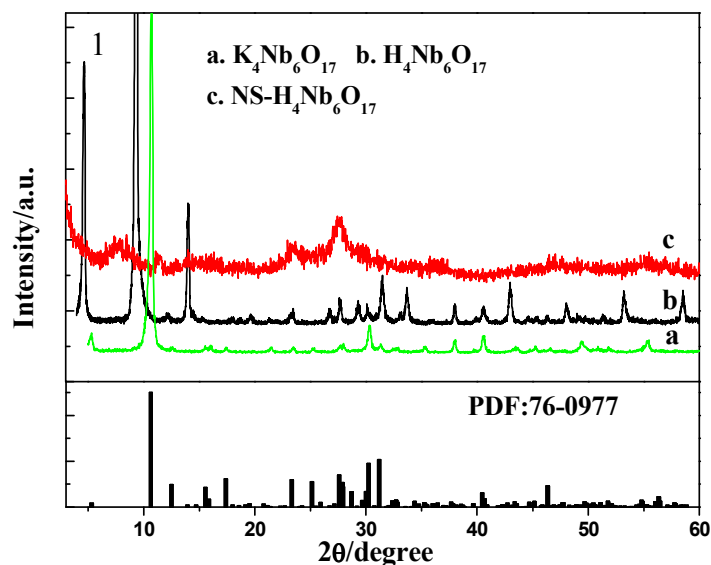


Fig.2 TG-DTA curves of composites before calcinations.

3.2 Structure and morphology characteristics of as-prepared samples

Fig.3 show the XRD patterns of as-prepared samples. For reference, K₄Nb₆O₁₇ and H₄Nb₆O₁₇ were characterized by XRD. The XRD pattern of K₄Nb₆O₁₇ sample is well matched with the standard spectra of K₄Nb₆O₁₇ (JCPDS 76-0799). As-prepared K₄Nb₆O₁₇ sample possesses a well-ordered layered orthorhombic phase structure. The diffraction peaks of 2θ = 5.33° and 10.66° belong to the (020) and (040) crystal plane, respectively. The *d*-spacing of (040) crystal plane is 0.83 nm using the Bragg equation $\lambda = 2d\sin\theta$. After ion-exchanging, due to the

existence of H_3O^+ in the interlayer, the (020) plane and (040) plane are shifted towards 4.67° and 9.33° from 5.33° and 10.66° , respectively. After exfoliation, the crystallinity of $\text{NS-H}_4\text{Nb}_6\text{O}_{17}$ descends evidently with the peak weaken and broaden, the peaks of (020) plane and (040) plane are disappeared, indicating that the layered structure is absent. The stronger peaks at 23.4° and 27.6° belong to (220) plane and (260) plane. From $\text{B-Fe}_2\text{O}_3/\text{Nb}_6\text{O}_{17}$ pattern, one can find the diffraction peaks at $2\theta = 32.6^\circ$ and 35.34° , which are the characteristic peaks of $\alpha\text{-Fe}_2\text{O}_3$ (PDF:33-0664), indicate that the as-prepared $\text{Fe}(\text{OH})_3$ sols have been partially crystallized into Fe_2O_3 crystal in the composite before it is calcinated. After $\text{B-Fe}_2\text{O}_3/\text{Nb}_6\text{O}_{17}$ was calcinated, the intensities of characteristic peaks of Fe_2O_3 are obviously enhanced, and the corresponding peak positions are shifted towards 32.9° and 35.74° , respectively. The average particle size of Fe_2O_3 before and after calcinations are 2.17 nm and 4.44 nm, respectively, using the Debye-Scherrer equation $D = k\lambda/B\cos\theta$. Considering the linear broadening caused by the instrument, the actual particle size of Fe_2O_3 is larger than the calculated value.



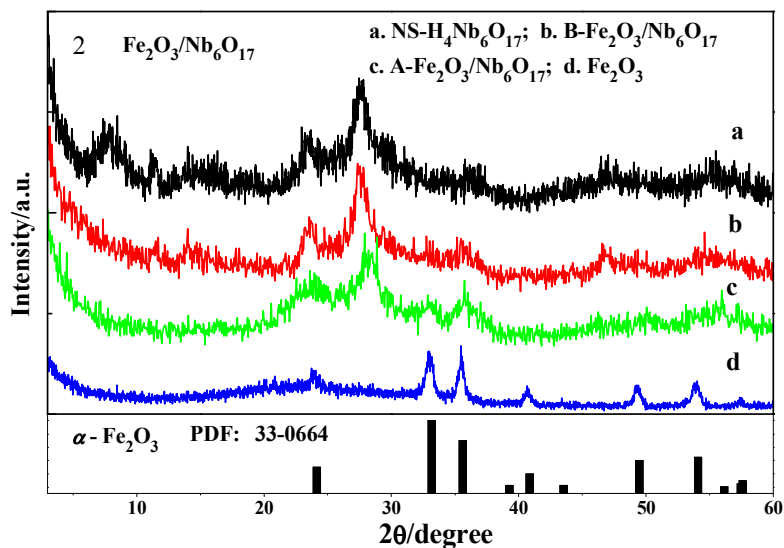
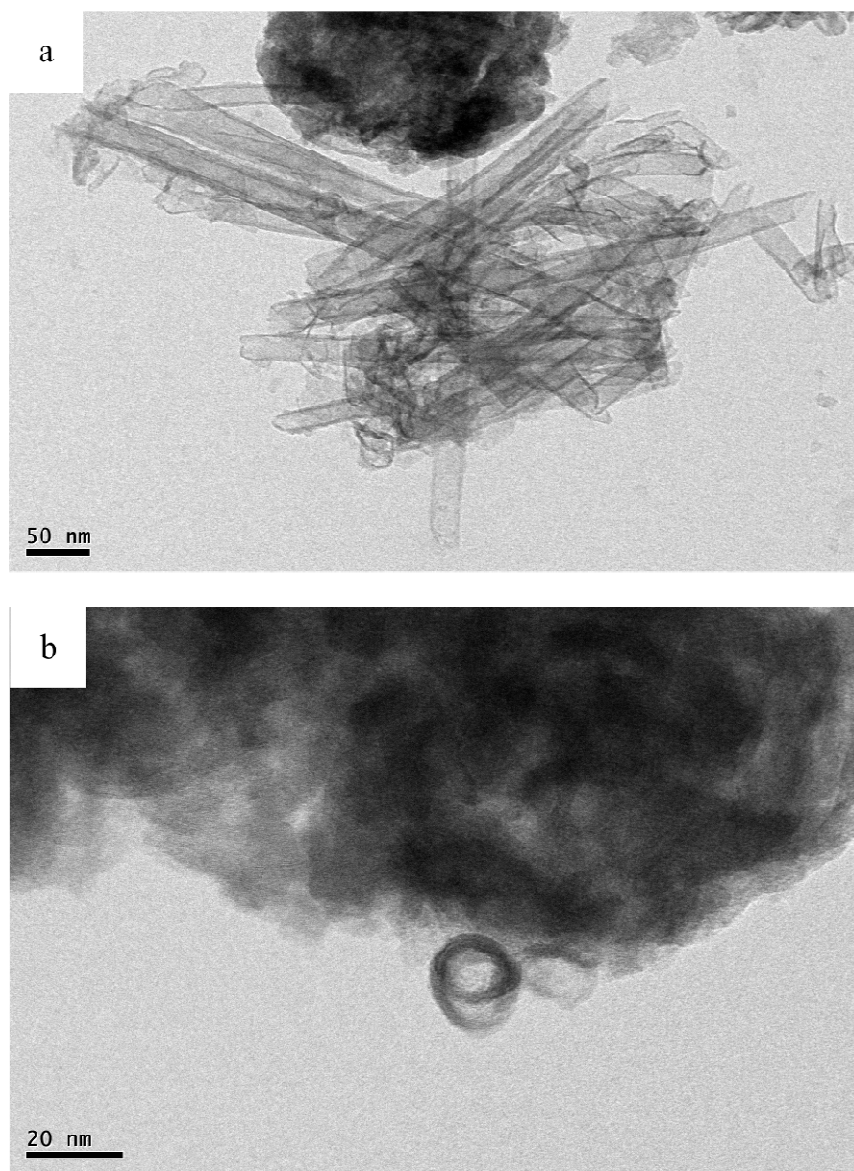
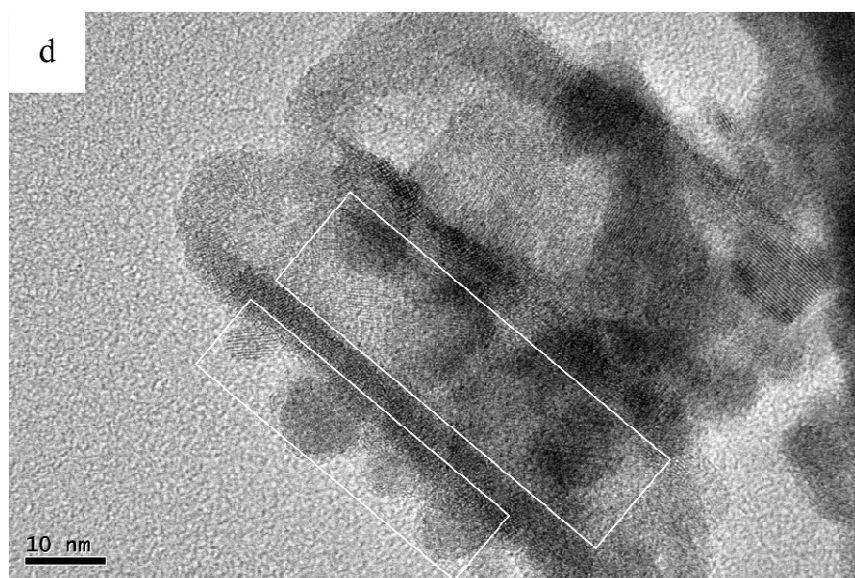
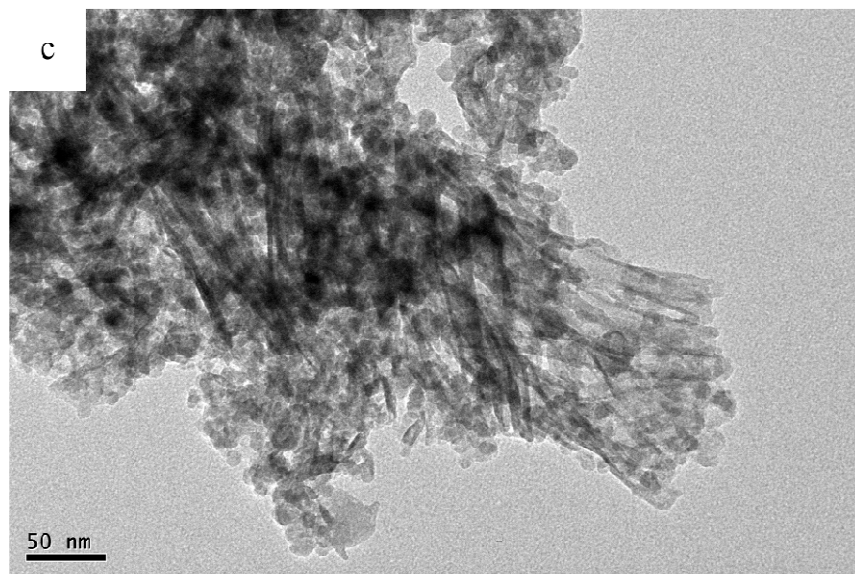


Fig.3 X-ray diffraction patterns of the as-prepared samples

The morphology of as-prepared samples was studied by FESEM and HRTEM technology, and the results are shown in Fig.4 and Fig.5. Some spherical particles randomly attached on the surface of nanoscrolls are clearly seen in the HRTEM images. It is well known that nanosheets have hydroxyl groups exposed at their surface. So the Fe(OH)₃ sols can react with hydroxyl groups on the surface of nanoscrolls to form Fe₂O₃ nanoparticles and attach to the surface of nanoscrolls. After calcination, Fe₂O₃ nanoparticles grew further, corresponding to the obtained result of the XRD patterns. The prepared nanoscroll composite stacks open before calcinations, and it becomes compact via calcinations, seen in Fig.4(supporting information). From Fig.5a and Fig.5c, it can be considered from the side that the calcination make the composite become tight and the nanoscroll owns well thermal stability. The HRTEM images of NS-H₄Nb₆O₁₇ indicate that tube-like structure is successfully prepared with the diameter of about 13~24 nm and the length of about 290~500 nm (Fig.5a). The lateral section of NS-H₄Nb₆O₁₇ (Fig.5b) possesses dark and bright field, suggesting the tube-like NS-H₄Nb₆O₁₇ owns the nanoscroll structure with the wall of varying thicknesses. When composited with Fe₂O₃ nanoparticles, typically spherical-shaped nanoparticles decorated on nanoscrolls are seen in Fig.5, and the Fe₂O₃ nanoparticles in these systems are distributed on the inside and outside walls of the nanoscrolls with different sizes in Fig.5d and Fig.5e. Fig.6 shows EDS spectra of NS-H₄Nb₆O₁₇ and A-Fe₂O₃/Nb₆O₁₇. From the

Fig.6a, one can find that the K^+ was completely removed from $NS-H_4Nb_6O_{17}$, and the mole ratio of Nb:O is about 1:4.2, the excess oxygen may be due to the adsorbed H_2O . The EDS spectrum reveals that the A- Fe_2O_3/Nb_6O_{17} nanoscroll composite contains iron. It is revealed that the composited nanoparticles belong to Fe_2O_3 based on the results of XRD. The mole ratio of Fe:Nb:O is about 1:1.6:4.8. It is clearly seen that the Fe element is partially lost in the prepared process, and the lower amount of oxygen may be owing to the chemical reaction between $Fe(OH)_3$ sols and nanoscrolls, and Nb-O-Fe may be formed.





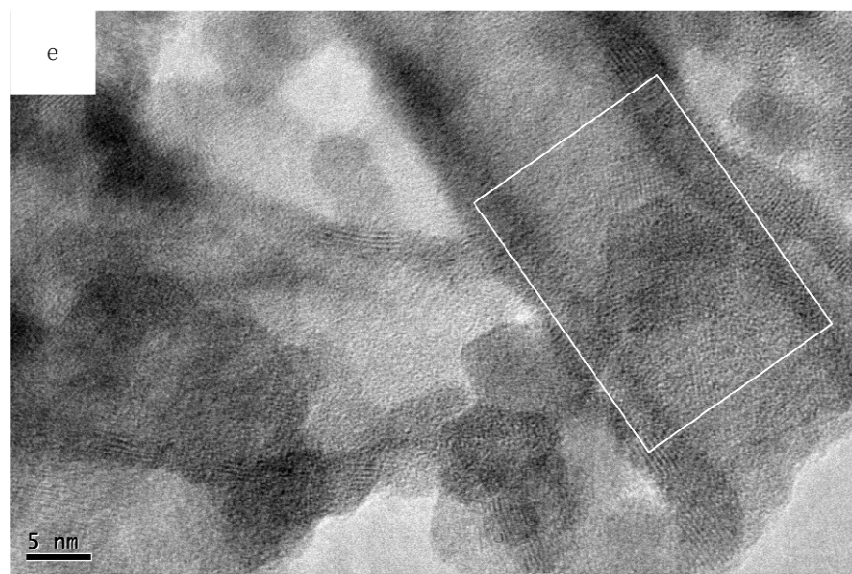


Fig.5 HRTEM images of the as-prepared samples(a and b. NS-H₄Nb₆O₁₇; c, d and e. A-Fe₂O₃/Nb₆O₁₇).

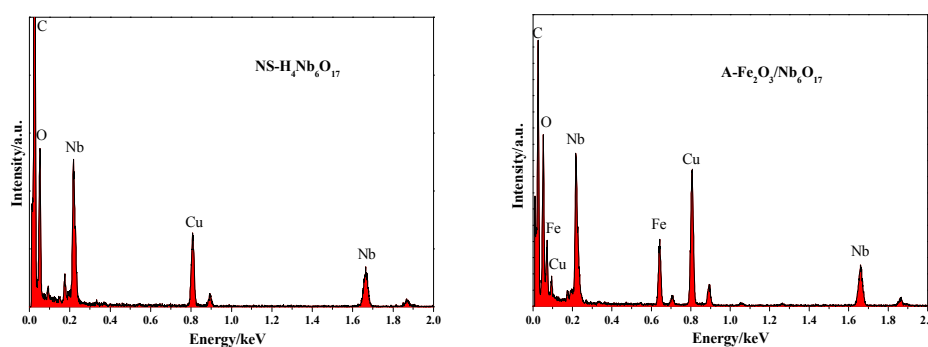


Fig.6 EDS spectra of NS-H₄Nb₆O₁₇ and A-Fe₂O₃/Nb₆O₁₇.

3.3 N₂ adsorption-desorption isotherms of as-prepared samples

N₂ adsorption-desorption isotherms of as-prepared samples are shown in Fig.7. The isotherms of the as-prepared samples exhibit a type IV isotherm due to the mesoporosity. As it can be seen, adsorption saturation is not reached in the range of higher relative pressure, all of them exhibit an IUPAC type H3 hysteresis loop in the range of 0.4~1.0, it may be ascribed to the existence of tube-shaped mesopores. From the Table 1, the BET specific surface area of the A-Fe₂O₃/Nb₆O₁₇ is 114 m²·g⁻¹, and ~2 times larger than that of NS-H₄Nb₆O₁₇ (64 m²·g⁻¹). The total pore volume of composites (0.41 cm³·g⁻¹) is larger than that of NS-H₄Nb₆O₁₇ (0.32 cm³·g⁻¹). This may be originated from assembling nanoscroll with oxide nanoparticles.

As it can be seen from the pore size distribution curves, both of them are consistent with mesoporous materials. The NS-H₄Nb₆O₁₇ shows two pore size distribution peaks with pore

diameter of ca. 3.7 nm and 13.2 nm. A mesoporous structure with the pore diameter of 3.7 nm, is still retained in composites. This may be the well-known artificial peak attribute to tensile strength effect^[21,22], which is disappeared for pore size distribution curve calculated by adsorption branches. And a broad peak with the pore diameter of 13.2 nm in the NS-H₄Nb₆O₁₇ may be attributed to diameter of nanoscroll structure, corresponding to the HRTEM of NS-H₄Nb₆O₁₇. After compositing with Fe₂O₃ nanoparticles, this broad peak with the pore diameter of 13.2 nm shifted to 8.5 nm may be derived from assembling nanoscroll with oxide nanoparticles, fractional nanoparticles are decorated on the inside surfaces of the nanoscrolls according to the HRTEM of A-Fe₂O₃/Nb₆O₁₇.

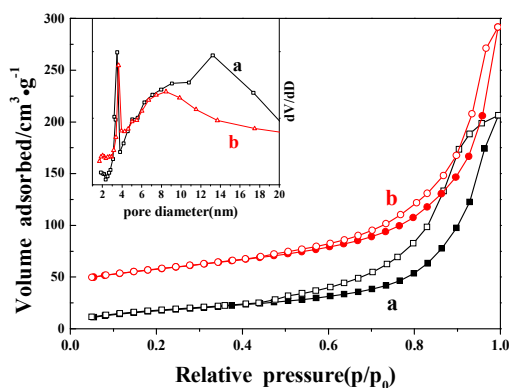


Fig. 7: N₂ adsorption-desorption isotherm of NS-H₄Nb₆O₁₇(a) and A-Fe₂O₃/Nb₆O₁₇(b). The inset indicates the pore size distribution curves.

Table 1 Parameters obtained from N₂ desorption measurements

Sample	Surface area ^a (m ² ·g ⁻¹)	Pore volume ^b (cm ³ ·g ⁻¹)
NS-H ₄ Nb ₆ O ₁₇	64	0.32
A-Fe ₂ O ₃ /Nb ₆ O ₁₇	114	0.41

^a BET specific surface area calculated from the linear part of BET plot.

^b Total pore volume taken from the volume of N₂ adsorbed at p/p₀ = 0.99.

3.4 Skeleton characteristics of as-prepared samples

The skeleton characteristics of composites were studied by Raman spectroscopy, which is shown in Fig.8. The strongest characteristic band of K₄Nb₆O₁₇ is around 877 cm⁻¹, which belongs to the stretching vibration of shorter Nb-O terminal group. The bands in 500-700 cm⁻¹ correspond

to the stretching vibrations of the longer Nb-O in NbO₆ octahedra unit. The other bands in 180-480 cm⁻¹ belong to the bending vibrations and librational modes of NbO₆ octahedra unit^[23]. A new Raman band exists at around 940 cm⁻¹ in the Raman spectrum of H₄Nb₆O₁₇ is attributed to the replacing of K⁺ by H₃O⁺ after the ion-exchange reaction, the terminal Nb-O bond become the Nb-O...H bond and further formed Nb-OH bond^[24].

In order to further investigate the interaction between nanoscroll support and Fe₂O₃ nanoparticle, the curves fitted from 1100 to 800 cm⁻¹ and 350 to 100 cm⁻¹ are also shown in Fig.8. The strong band around 881 cm⁻¹ in the Raman spectra of NS-H₄Nb₆O₁₇ is assigned to stretching vibration of shorter Nb-O terminal group. A shoulder band at 928 cm⁻¹ is assigned to Nb-OH bond driven from hydrous shorter Nb-O terminal group. The bands at 145 cm⁻¹ may be due to the contribution of translational motions of the Nb atoms. When the nanoscroll composited with Fe(OH)₃ sols, the Nb-OH bond is blue-shifted to 935 cm⁻¹ in B-Fe₂O₃/Nb₆O₁₇. The result indicates that the Fe(OH)₃ sols have interacted with Nb-OH bonds. The bands at 268 cm⁻¹ have disappeared while a new broaden band has emerged at 274 cm⁻¹. The later band may be a merged band composed of the band of crystalline Fe₂O₃ nanoparticles and the band of NS-H₄Nb₆O₁₇ at 268 cm⁻¹. The bands at 224 cm⁻¹ and 295 cm⁻¹, corresponding to the band of α-Fe₂O₃ in A-Fe₂O₃/Nb₆O₁₇, are blue-shifted ca. 5 cm⁻¹ and 10 cm⁻¹ compared to pure α-Fe₂O₃, respectively. This corresponded to an XRD-pattern which parameters have slightly changed. The Nb-OH bond is further blue-shifted to 953 cm⁻¹, and the Nb-O terminal band is blue-shifted to 897 cm⁻¹, the intensities of Nb-O terminal bond and Nb-OH bond are weaken obviously. Due to the higher electronegativity of Fe as compared to Nb, the strength of the Nb-O bond is enhanced and blue-shifted. So the interaction between Fe₂O₃ and nanoscrolls are obviously enhanced, and the chemical band of Nb-O-Fe may be formed. Further analysis points out that there exists a new broaden band at 239 cm⁻¹ in A-Fe₂O₃/Nb₆O₁₇, which is also assigned to the merged band between the band of NS-H₄Nb₆O₁₇ at 268 cm⁻¹ and 209 cm⁻¹.

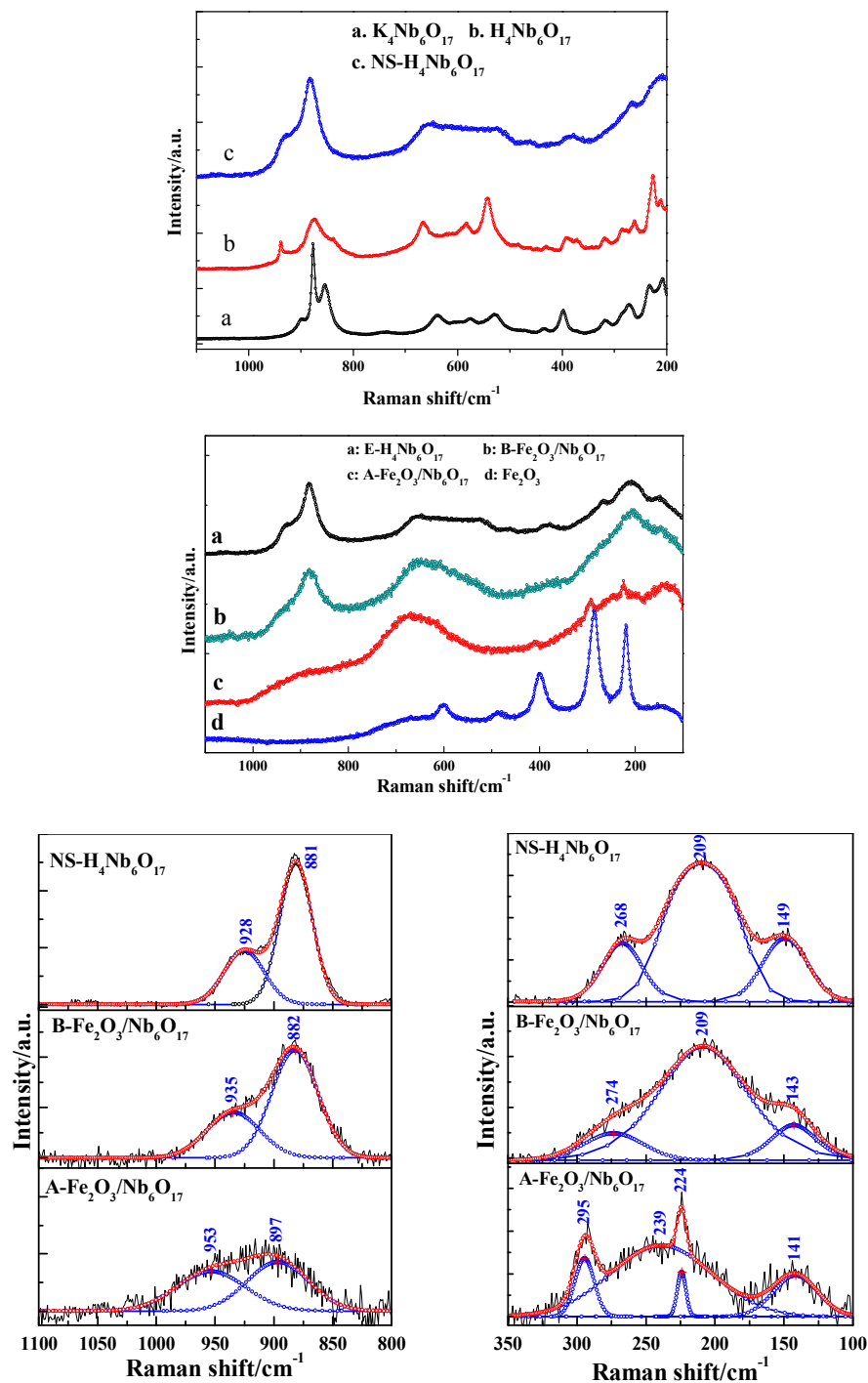


Fig.8 Raman spectra and fitted curves of as-prepared samples.

3.5 Optical characterization of as-prepared samples

The spectral response characteristics of as-prepared samples was investigated by the method of UV-vis DRS, and results are shown in Fig.9. The analysed results are displayed in Table 2 using the equation $\Delta E = 1240 / \lambda$ (nm). Obvious red shifts are observed for the $\text{B-Fe}_2\text{O}_3/\text{Nb}_6\text{O}_{17}$

and A-Fe₂O₃/Nb₆O₁₇ (with the band gap of 1.86 eV and 1.82 eV, respectively), indicating that the introduced Fe₂O₃ nanoparticles decline the band gap of the composites and the interaction between Fe₂O₃ nanoparticles and nanoscrolls are existed in composites. The absorption edge of Fe₂O₃/Nb₆O₁₇ composites only exhibit slight variation before and after calcinations (band gap from 1.86 eV to 1.82 eV). It may be explained the B-Fe₂O₃/Nb₆O₁₇ owns relatively stronger interaction and Fe(OH)₃ sols were partially turned into Fe₂O₃ crystal, the calcination is inadequate to significantly adjust the band gap of samples.

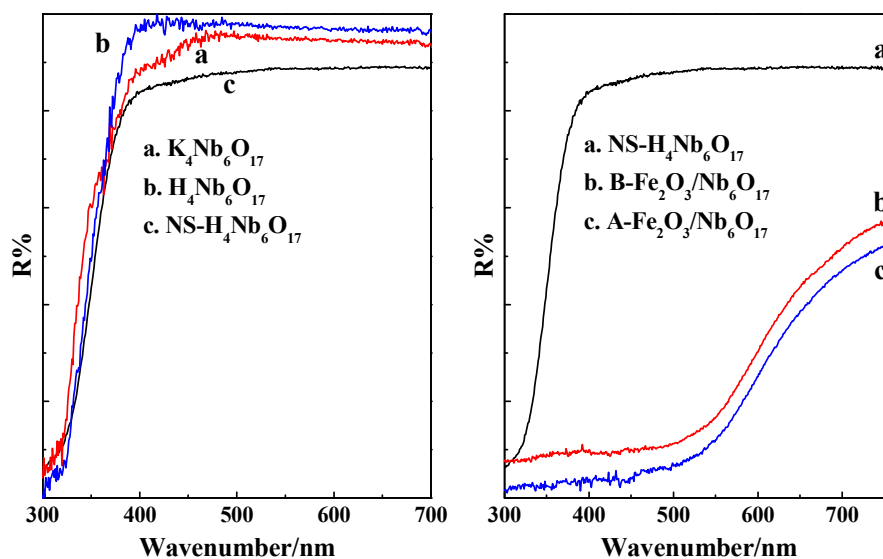


Fig.9 UV-vis-DRS of as-prepared samples.

Table 2 The absorption edge and the band gap energy of as-prepared samples.

Samples	Absorption edge(λ /nm)	Band gap/eV
K ₄ Nb ₆ O ₁₇	400	3.10
H ₄ Nb ₆ O ₁₇	390	3.18
NS-H ₄ Nb ₆ O ₁₇	380	3.26
B-Fe ₂ O ₃ /Nb ₆ O ₁₇	667	1.86
A-Fe ₂ O ₃ /Nb ₆ O ₁₇	680	1.82

3.6 Photocatalytic activity

The photocatalytic activity of as-prepared samples was evaluated from the rate of photodegradation of MB under visible light irradiation (Fig.10). As it can be seen, the degradation

rates of MB over the as-prepared composites (~77% and ~85% after 240 min, respectively) are much higher than that over NS- $\text{H}_4\text{Nb}_6\text{O}_{17}$ and Fe_2O_3 (~45% and 63% after 240min, respectively). It may be because the composites have stronger visible light absorption capacity, larger specific surface areas. The rate of MB degradation over A- $\text{Fe}_2\text{O}_3/\text{Nb}_6\text{O}_{17}$ is slightly higher than that over B- $\text{Fe}_2\text{O}_3/\text{Nb}_6\text{O}_{17}$, which may be due to the enhanced interaction after calcinations.

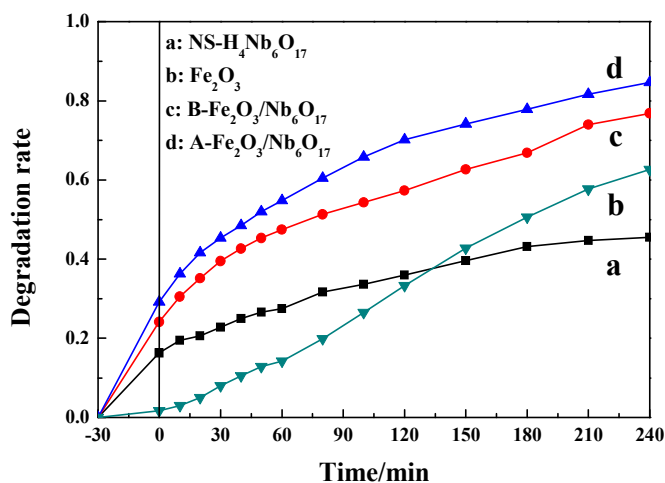


Fig.10 The photocatalytic degradation of MB over the as-prepared samples under visible light ($\lambda > 400$ nm) irradiation.

3.7 Possible assembly mechanism

The prepared process of composites is schematically illustrated in Fig.11. According to the HRTEM, the Fe_2O_3 nanoparticles are distributed on the inside and outside surfaces of the nanoscrolls. A mass of hydroxyl groups (such as Nb-OH), which is well known, are exposed at the surface of nanoscrolls. The hydroxyl groups Nb-OH can be formed by the hydrous terminal Nb-O \cdots H $_2$ O groups. The “hydroxyl titration” model suppose that the surface metal oxide species primarily coordinate to the oxide supports by titrating the surface hydroxyls of the supports^[25]. Previous studies^[26] have shown that $\text{Nb}_2\text{O}_5/\text{SiO}_2$ was prepared by cross-condensation of surface hydroxyl groups of the SiO_2 support with the surface hydroxyl entities of Nb_2O_5 , and the surface hydroxyl groups of SiO_2 support with stronger activity are easier to react with niobia species. Due to higher acidity of niobate, cross-condensation of the hydroxyl entities of Fe_2O_3 with Nb_6O_{17} is potentially easier. Considering the result above-mentioned in the Raman of the as-prepared composites that the terminal Nb-O band and terminal hydroxyl groups (Nb-OH) are obviously

weaken and shifted, the terminal hydroxyl groups (Nb-OH) may own stronger activity to interact with the oxide sols. So the terminal hydroxyl groups (Nb-OH) may become the active sites of dispersing oxide nanoparticles. However, the interactions between oxide sols and nanoscrolls are relatively weak before calcinations. When the composite is calcined, the reaction between hydroxyl groups of oxide sols and nanoscrolls is enhanced. At the meantime, the oxide sols further turned into oxide nanoparticles, and the oxide nanoparticles continued to grow.

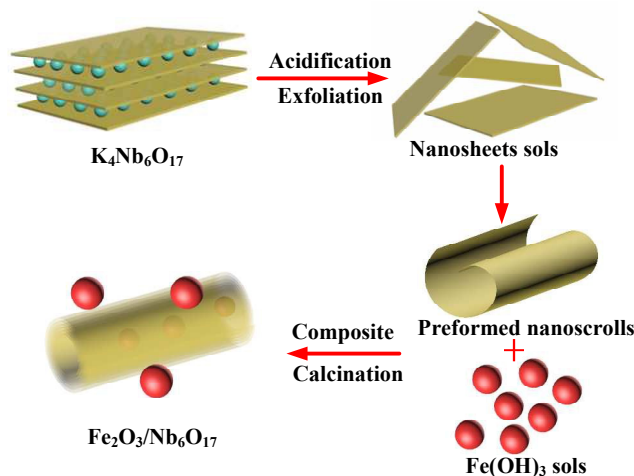


Fig.11 Schematic diagram of assembly mechanism for composite.

4. Conclusion

Composites are successfully prepared via combining the nanoscrolls sols with oxide sols at moderate conditions. Fe_2O_3 nanoparticles are distributed on the inside and outside surfaces of the nanoscrolls with different sizes. The pore volumes and specific surface areas are increased. The absorption edge of the as-prepared composites exist apparent red shift compared to support NS- $H_4Nb_6O_{17}$. The absorption edge of A- Fe_2O_3/Nb_6O_{17} was further red-shifted compared to B- Fe_2O_3/Nb_6O_{17} due to the enhanced interactions. It has a very promising application in the photocatalytic field. The work reveals that the composite own strong interactions between oxide and nanoscrolls via combining oxide with Nb-OH terminal band. An assembly mechanism of nanoscroll with oxide nanoparticles is supposed through scrolling the exfoliated $Nb_6O_{17}^{4-}$ nanosheets sols into nanoscrolls prior to assembly. The surface hydroxyl groups of nanoscrolls play important role in compositing with oxide nanoparticles.

Acknowledgements

This work was supported by the Natural Science Foundation of China (no. 21271008, 21071004), Anhui Provincial Natural Science Foundation (no. 11040606M38).

Reference

- 1 X. Peng, L. L. Peng, C. Z. Wu and Y. Xie, *Chem Soc Rev*, 2014, **43**, 3303.
- 2 A. S. Dias, S. Lima, D. Carriazo, V. Rives, M. Pillinger and A. A. Valente, *J. Catal.*, 2006, **244**, 230.
- 3 M. A. Bizeto, A. L. Shiguihara and V. R. L. Constantino, *J. Mater. Chem.*, 2009, **19**, 2512.
- 4 Y. Yamada, A. Nomura, H. Tadokoro and S. Fukuzumi, *Catal. Sci. Technol.*, 2015, **5**, 428.
- 5 M. Osada and T. Sasaki, *ECS Transaction*, 2012, **50**, 111.
- 6 K. Maeda, G. Sahara, M. Eguchi and O. Ishitani, *ACS Catal.*, 2015, **5**, 1700.
- 7 C. Zhou, Y. F. Zhao, L. Shang, Y. H. Cao, L. Z. Wu, C. H. Tung and T. R. Zhang, *Chem. Commun.*, 2014, **50**, 9554.
- 8 W. Q. Cui, M. Y. Shao, L. Liu, Y. H. Liang and D. Rana, *Appl. Surf. Sci.*, 2013, **276**, 823.
- 9 X. Q. Li, T. Y. Zhang, S. W. Gu, S. Z. Kang, G. D. Li and J. Mu, *Sep. Purif. Technol.*, 2013, **108**, 139.
- 10 X. T. Pian, B. Z. Lin, Y. L. Chen, J. D. Kuang, K. Z. Zhang and L.M.Fu, *J. Phys. Chem. C*, 2011, **115**, 6531.
- 11 S. Adireddy, Y. Yao, J. B. He and J. B. Wiley, *Mater. Res. Bull.*, 2013, **48**, 3236.
- 12 Y. Yao, G. S. Chaubey and J. B. Wiley, *J. Am. Chem. Soc.*, 2012, **134**, 2450.
- 13 S. Adireddy, C. E. Carbo, Y. Yao, J. M. Vargas, L. Spinu and J. B. Wiley, *Chem. Mater.*, 2013, **25**, 3902.
- 14 S. Adireddy, T. Rostamzadeh, C. E. Carbo and J. B. Wiley, *Langmuir*, 2015, **31**, 480.
- 15 F. E. Sarac, C. Yilmaz, F. Y. Acar And U. Unal, *RSC Adv.*, 2012, **2**, 10182.
- 16 C. H. Hu, L. H. Zhang, J. F. Zhang, L. Y. Cheng, Z. Zhai, J. Chen and W. H. Hou, *Appl. Surf.*

- Sci., 2014, **298**, 116.
- 17 S. Adireddy, C. E. Carbo, T. Rostamzadeh, J. M. Vargas, L. Spinu and J. B. Wiley, *Angew. Chem. Int. Ed.*, 2014, **53**, 4614.
- 18 R. Ma, Y. Kobayashi, W. J. Youngblood and T. E. Mallouk, *J. Mater. Chem.*, 2008, **18**, 5982.
- 19 T. K. Townsend, E. M. Sabio, N. D. Browning and F. E. Osterloh, *ChemSusChem*, 2011, **4**, 185.
- 20 Z. J. Chen, B. H. Lin, Y. L. Chen, K. Z. Zhang, B. Li and H. Zhu, *J. Phys. Chem. Solids*, 2010, **71**, 841.
- 21 J. C. Groen, L. A. A. Peffer and J. Pérez-Ramírez, *Microporous Mesoporous Mater.*, 2003, **60**, 1–17.
- 22 C. Hu and L. Zhang, *J. Energy Chem.*, 2014, **23**, 136–144.
- 23 M. Mączka, M. Ptak, A. Majchrowski and J. Hanuza, *J. Raman Spectrosc.*, 2011, **42**, 209–213.
- 24 Y. Hosogi, H. Kato and A. Kudo, *J. Phys. Chem. C*, 2008, **112**, 17678–17682.
- 25 I. E. Wachs, *Catal. Today*, 1996, **27**, 437.
- 26 J. He, Q. J. Li and Y. N. Fan, *J. Solid State Chem.*, 2013, **202**, 121.

List

- Fig.1: Structure diagram of $K_4Nb_6O_{17}$.
- Fig.2: TG-DTA curves of composites before calcinations.
- Fig.3: X-ray diffraction patterns of the as-prepared samples.
- Fig.4: Field emission scanning electron microscopy (FESEM) images of the as-prepared samples(a. B- Fe_2O_3/Nb_6O_{17} ; b. A- Fe_2O_3/Nb_6O_{17}).
- Fig.5: HRTEM images of the as-prepared samples(a.b. NS- $H_4Nb_6O_{17}$; c, d and e. A- Fe_2O_3/Nb_6O_{17}).
- Fig.6: EDS spectra of NS- $H_4Nb_6O_{17}$ and A- Fe_2O_3/Nb_6O_{17} .

Fig.7: N₂ adsorption-desorption isotherm of NS-H₄Nb₆O₁₇(a) and A-Fe₂O₃/Nb₆O₁₇(b).

The inset indicates the pore size distribution curves.

Fig.8: Raman spectra and fitted curves of as-prepared samples.

Fig.9: UV-vis-DRS of as-prepared samples.

Fig.10: The photocatalytic degradation of MB over the as-prepared samples under visible light ($\lambda > 400$ nm) irradiation.

Fig.11 Schematic diagram of assembly mechanism for composite.

Table 1: Parameters obtained from N₂ desorption measurements.

Table 2: The absorption edge and the band gap energy of as-prepared samples.

Fe_2O_3 nanoparticles are crosslinked to the niobate nanoscroll surface by associated with terminal Nb-OH groups.

